ARTICLES

Photofragment Translational Spectroscopy of *n*-C_3H_7I and *i*-C_3H_7I near 280 and 304 nm

Xiling Xu, Zijun Yu, Weibin Bi, Daoqing Xiao, Dan Yu, Yikui Du,* and Qihe Zhu*

Beijing National Laboratory for Molecular Sciences, State Key Laboratory of Molecular Reaction Dynamics, Institute of Chemistry, Chinese Academy of Sciences, Beijing 100080, P. R. China

Received: July 20, 2007; In Final Form: December 29, 2007

The photodissociation dynamics of propyl iodides *n*-C_3H_7I and *i*-C_3H_7I near 280 and 304 nm has been investigated with our mini-TOF photofragment translational spectrometer. When a single laser is applied for both the photodissociation of parent molecules and the REMPI of I atom photofragments, the TOF spectra of photofragments I*($^2P_{1/2}$) and I ($^2P_{3/2}$) are obtained at four different wavelengths for these two iodides. For *n*-C_3H_7I, some small vibrational peaks are partially resolved (with separation of ∼522 cm^{-1}, corresponding to the RCH_2 deformation frequency of the fragment *n*-C_3H_7) at 281.73, 279.71, and 304.67 nm. These results show that the RCH_2 deformation is mostly excited. For *i*-C_3H_7I, we obtain some partially resolved vibrational peaks (with separation of ∼352 cm^{-1}, corresponding to the $HC(CH_3)_2$ out-of-plane bending frequency of the fragment *i*-C_3H_7) at 281.73 nm only. For *n*-C_3H_7I, the partitioning values of the available energy $\bar{E}_{int}/E_{avl}$ are 0.48 at 281.73 nm and 0.49 at 304.02 nm for the I* channel, and 0.52 at both 279.71 and 304.67 nm for the I channel. These energy partitioning values are comparable with the previous results at different wavelengths in the literature. For *i*-C_3H_7I, the $\bar{E}_{int}/E_{avl}$ values are 0.61 at 281.73 nm, 0.65 at 304.02 nm for the I* channel, and 0.62 at 279.71 nm, 0.49 at 304.67 nm for the I channel. The potential-energy-surface crossing and the β values have also been discussed.

1. Introduction

The photofragment translational spectroscopy (PTS) is an important method for the study on the photodissociation dynamics of simple polyatomic molecules, and the resolution of PTS has been continuously improved. Studies with high-resolution PTS can usually provide more detailed information for the photodissociation dynamics.

The photodissociation dynamics of alkyl iodides and fluorinated alkyl iodides in the A band absorption has been intensively investigated for several decades. The vibrational-state-resolved high-resolution photofragment translational spectra can be achieved from alkyl iodides more easily than from alkyl chlorides and alkyl bromides, because the breaking of the C−I bond of alkyl iodides is easier than that of the C−Cl and C−Br bond, the spin−orbit splitting energy of I*/I is higher than those of Cl*/Cl and Br*/Br, and there is only one stable isotope of iodine. The A band of alkyl iodides is a continuous absorption band that arises from a transition of a nonbonding electron of iodine to the antibonding σ^* orbital of the C−I bond. The A band is composed of three excited states $^3Q_1$, $^3Q_0$, and $^1Q_1$ (denoted by Mulliken[1] in increasing energy order). The $^3Q_0$ state correlates adiabatically with the spin−orbit excited state I*($^2P_{1/2}$) and the $^3Q_1$ and $^1Q_1$ states correlate with the ground state I ($^2P_{3/2}$).

Among alkyl iodides, CH_3I[2−10] and CF_3I[11−22] have been studied most intensively, because they are the simplest iodides and can be taken as the pseudo-triatomic molecules. Using the conventional photofragment translational spectrometer, Y. T. Lee's group[23] resolved the ν_2 umbrella vibrational states of CH_3 photofragment from CH_3I at 248 nm; Felder[11] and Wang et al.[20] resolved some ν_2 umbrella vibrational states of CF_3 from CF_3I at 248 nm. Using velocity map imaging, Eppink et al.[3,7] resolved the ν_2 umbrella vibrational states of CH_3 in the wavelength region from 222 to 333 nm and Aguirre et al.[19] resolved the ν_2 umbrella vibrational states of CF_3 between 277 and 304 nm. Using a mini-TOF photofragment translational spectrometer (weak field acceleration), Tian et al.[21] resolved different ν_2 umbrella vibrational states of CF_3 at 281.73 nm. Recently, using long time-delayed core-sampling PTS,[24] Li and co-workers[10,22] resolved the ν_2 umbrella vibrational states of CH_3 and CF_3 near 304 nm. However, the investigations on the more complex alkyl iodides with high-resolution PTS are still less. For the photodissociation of C_2H_5I, Bi et al.[25] resolved some ν_2 CCH_2 umbrella vibrational states of photofragment C_2H_5 at four different wavelengths near 280 nm and 304 nm with our mini-TOF photofragment translational spectrometer.

As for *n*-C_3H_7I and *i*-C_3H_7I, Riley et al.[2] studied their photodissociation at 266 nm and Godwin et al.[26] studied their photodissociation at 248 nm using conventional photofragment translational spectrometer, but they could not resolve the I* and I dissociation channels. Zhu et al.[5] performed similar experiments at 248 nm and resolved clearly the two channels. Kang et al.[6] got the energy partitioning of *n*-C_3H_7I for the I* and I channels near 304 nm by PTS with delayed acceleration. Recently, Fan et al.[27] used velocity map imaging to study the

* Corresponding authors. E-mail: Y.D., ydu@iccas.ac.cn; Q.Z., qhzhu@iccas.ac.cn.

10.1021/jp0756956 CCC: $40.75
Published on Web 02/13/2008

internal energy dependence of the relative photoionization yields of the n-C_3H_7 and i-C_3H_7 radicals from the 266 nm photodissociation of the propyl iodides. In all these photodissociation studies of propyl iodides, the vibrational states of propyl radicals were not even partially resolved.

In this paper, we report the study on the photodissociation dynamics of n-C_3H_7I and i-C_3H_7I at 281.73 and 304.02 nm for the I* channel and at 279.71 and 304.67 nm for the I channel by the mini-TOF photofragment translational spectrometer using weak field acceleration. We hope to resolve the vibrational states of propyl radicals, to get more reliable energy partitioning and other information of photodissociation dynamics.

2. Experimental Section

The experimental apparatus has been described in detail elsewhere.[21,25] Briefly, it consists of a source chamber and a reaction chamber. In the source chamber, there is a pulse valve (General Valve, 0.5 mm diameter orifice), operated at 10 Hz with pulse duration of about 300 μs. The two chambers are pumped by turbomolecular pumps (600 L/s). During the operation of the pulse valve, the pressure of the source chamber increases from 1×10^{-5} to 3×10^{-3} Pa, and the pressure of the reaction chamber remains at about 1×10^{-5} Pa. The samples n-C_3H_7I (AR, 99%) and i-C_3H_7I (AR, >98%) are used directly without further purification. The carrier gas Kr of 1 atm is bubbled through the liquid sample to form the gas mixture. The application of the heavier carrier gas Kr can lower the velocity of the molecular beam (MB), and then the velocity spread of the molecular beam will be lower than that with lighter carrier gas. This will decrease the unfavorable effect to the resolution of the PTS experiments. The gaseous sample is supersonically expanded via the nozzle of the pulse valve into the source chamber. The cooled molecules along the central axis pass through a skimmer of 0.5 mm diameter, localized 20 mm downstream from the nozzle of the pulse valve, forming a supersonic molecular beam in the reaction chamber.

The UV laser light used is the second harmonic of a dye laser (Quanta-Ray, PDL-2) pumped by a YAG laser (Quanta-Ray, Pro 230) at a repetition rate of 10 Hz. The dye Rhodamine 590 (Exciton) is used for the UV laser of 281.73 or 279.71 nm and Rhodamine 640 (Exciton) for 304.02 or 304.67 nm. The UV laser, focused with a quartz lens (75 mm focal length), intersects perpendicularly with the front portion of the molecular beam in the reaction chamber, 90 mm from the hole of the skimmer. The same laser pulse is used both for the photodissociation of the parent molecules and for the (2 + 1) resonance-enhanced multiphoton ionization (REMPI) of the photofragments I* or I. The wavelengths are 281.73 nm (6p ($2^0_{3/2}$) ← $5p^5$ ($^2P^0_{1/2}$)) and 304.02 nm (6p ($^4D^0_{1/2}$) ← $5p^5$ ($^2P^0_{1/2}$)) for the I* channel and 279.71 nm (6p ($^2P^0_{1/2}$) ← $5p^5$ ($^2P^0_{3/2}$)) and 304.67 nm (6p ($^2D^0_{5/2}$) ← $5p^5$ ($^2P^0_{3/2}$)) for the I channel.[28] To minimize the space charge effect between the ionized photofragments, the UV laser power is tuned as low as between 0.05 and 0.25 mJ per pulse. The laser power is different for different wavelength but is kept constant for one wavelength. The polarization of the laser is turned to be parallel to the acceleration field E for the experiments of Figures 2−6.

The fragment ions I^+ are accelerated by a weak electric field for a length l_1 and then fly freely in a region of length L_2 (see Figure 1). The I^+ ions form a Newton sphere in region L_1 and become a discus-like ellipsoid in region L_2. The lengths l_1 = 16 mm and L_2 = 34 mm are taken to satisfy approximately the first-order space focus condition:[29]

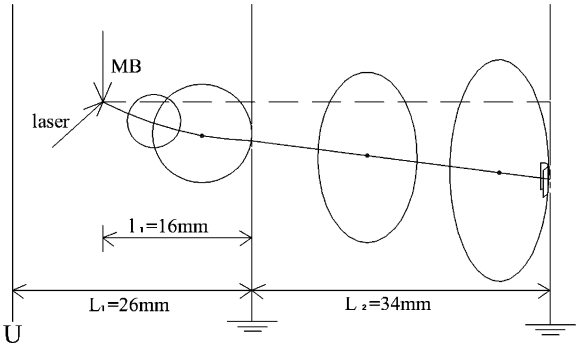

Figure 1. Schematic diagram of the flight path of photofragment ions.

$$^1/_2 m_I V_{CM}^{\ 2} + qEl_1 = {}^1/_2 qEL_2 \quad (1a)$$

$$E = U/L_1 \quad (1b)$$

where m_I is the mass of the iodine ion, V_{CM} is the center-of-mass velocity of the iodine photofragment, q is the charge of the I^+ ion, E is the electric field strength in region L_1, and U is the dc voltage on the repeller plate.

We adopt a rectangular detection hole (with a screen) of 8 × 20 mm^2 in size, and its long edge is circular in shape with a curvature of R = 31 mm. This cylindrical detection hole will increase the sensitivity without loss in resolution. The purpose of using different voltage U on the repeller plate at different wavelengths is to satisfy the space focus condition and to make the front Newton surface of the final discus-like ellipsoid in region L_2 (Figure 1) coincident with the cylindrical detection hole.

In the detector region, we put an extra grid plate of low voltage (−25 V) between the grounded detection plate and the high-voltage (−2 kV) microchannel plate (MCP). This will prevent the strong electric field to penetrate through the screen on the detection hole into the free drift region L_2, so that the resolution can be improved. The signals from the MCP are preamplified and recorded by a 500 MHz multichannel scaler (Fast, P7888-1(E)). The time sequence of the Nd:YAG laser, the pulsed valve, and the multichannel scaler is controlled by a digital delay/pulse generator (Stanford Research Systems, DG535).

3. Results and Discussion

From the photofragment translational spectroscopy, one can study the partitioning of the available energy into the translational energy and the internal energy of the photofragments. With the high-resolution PTS, one can resolve the vibrational states of the photofragments and understand the selective excitation of the vibrational modes.

There are two dissociation channels for each propyl iodide,

$$RI \xrightarrow{h\nu} R(v,j) + I^*$$
$$R(v',j') + I$$

These two channels can be detected separately using different REMPI wavelengths of I* and I.

The available energy E_{avl} can be calculated from the conservation of energy:

$$h\nu + E_{int}(RI) = D_0(C{-}I) + E_{so} + E_{int}(R) + E_T \quad (2)$$

$$E_{avl} = E_{int}(R) + E_T = h\nu + E_{int}(RI) - D_0(C{-}I) - E_{so} \quad (3)$$

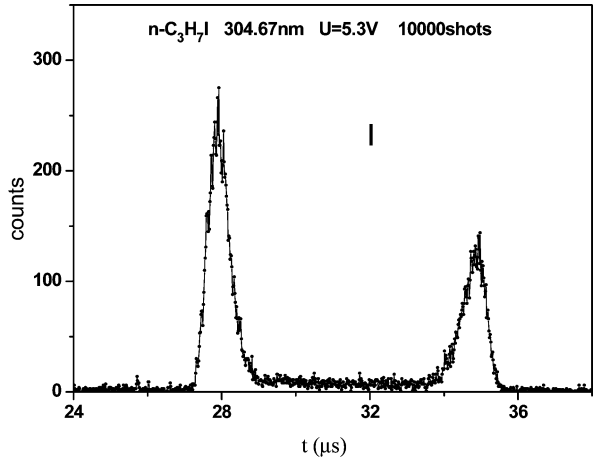

Figure 2. Typical TOF spectrum of resonantly ionized I from the photodissociation of n-C_3H_7I at 304.67 nm (repeller $U = 5.3$ V, channel width 16 ns, 10 000 laser shots).

where $h\nu$ is the photon energy of the dissociation laser, E_{int}(RI) is the internal energy of the parent molecule, which can be generally neglected due to the lower temperature of the supersonic molecular beam, D_0(C−I) is the C−I bond dissociation energy (for comparison with previous results, we use the old values: $D_0 = 2.363$ eV for n-C_3H_7I[26] and $D_0 = 2.296$ eV for i-C_3H_7I[26]), E_{so}= 0.943 eV is the spin−orbit splitting energy of iodine atom for the I* channel and is discarded for the I channel, E_{int}(R) is the internal energy of the propyl radical, and E_T is the total translational energy of two photofragments.

The translational energy distribution can be obtained from the experimental TOF spectrum of I^+ ions with the following formulas:

$$V_{CM} = a\left(\frac{t}{2}\right) = \frac{qE}{m_I}\left(\frac{t}{2}\right) = \frac{q}{m_I}\frac{U}{L_1}\left(\frac{t}{2}\right) \quad (4)$$

$$E_T = \frac{1}{2} m_I {V_{CM}}^2 \left(\frac{m_R + m_I}{m_R}\right) \quad (5)$$

where a is the acceleration of I^+ in region L_1, t is the turn-around time of iodine ions (with V_{CM} and E in opposite direction) that can be obtained from the TOF spectrum, and m_R is the mass of the propyl radical. The variation of the equivalent solid angle of the detection hole for the acceptance of ions with different V_{CM} is also considered.

3.1. Photodissociation of n-C_3H_7I. The complete TOF spectrum of the ionized I from the photodissociation of n-C_3H_7I at 304.67 nm is shown in Figure 2 as an example. The laser is polarized parallel to the acceleration field. The two broad TOF peaks correspond to the recoil velocity distribution of iodine fragments with opposite recoil directions. For the earlier peak, the direction of the recoil velocity is the same as that of the acceleration field, directing toward the MCP detector. For the later peak, the recoil velocity is directing opposite to the acceleration field, but these ions turn around due to the field and then fly toward the MCP detector. The earlier peak is selected for analysis, because the experimental conditions (especially the cylindrical detection hole) are optimized for this peak. The spectra in Figure 3a−d show the enlarged earlier peaks of the TOF spectra for I* at 281.73 and 304.02 nm and for I at 279.71 and 304.67 nm, respectively. The corresponding translational energy distributions of the photofragments are shown in Figure 4a−d, respectively.

In Figure 3a,c,d and Figure 4a,c,d, i.e. at 281.73, 279.71, and 304.67 nm, some small vibrational peaks are partially resolved with the separation of about 522 cm^{-1}, corresponding to the vibrational frequency 530 cm^{-1} of the RCH_2 deformation of n-C_3H_7 free radical.[30] (Only the spectrum at 304.02 nm in Figure 3b is not vibrationally resolved due to the very weak signal.) During the C−I bond breaking of n-C_3H_7I, the α-carbon experiences the strongest force, and the three atoms attached to the α-carbon also experience some strong effect. Hence, the vibrational mode of RCH_2 deformation in the fragment n-C_3H_7 might be excited more strongly than other vibrational modes during bond breaking, just as we have observed in our experiments. However, we cannot assign exactly the vibrational states in the TOF spectra, because some other vibrational modes might also be excited when E_{avl} is quite high. In Figure 3a,c,d and Figure 4a,c,d, we have given the small peaks some quantum numbers v of the RCH_2 deformation vibrational mode (supposing no other vibrational excitation), just to show the extent of the internal energy excitation.

The average value of the translational energy $\bar{E}_T$ can be derived from the translational energy distribution. Then, the fraction of the internal energy in the available energy can be obtained from formula 6

$$\frac{\bar{E}_{int}}{E_{avl}} = \frac{E_{avl} - \bar{E}_T}{E_{avl}} \quad (6)$$

Table 1 displays the values of energy partitioning for the photodissociation of n-C_3H_7I. For the I* channel, we obtain $\bar{E}_{int}/E_{avl} = 0.48$ at 281.73 nm and 0.49 at 304.02 nm, comparable to the previous results at 248, 266, and 304.02 nm. Our new results also show that the energy partitioning $\bar{E}_{int}/E_{avl}$ does not change much with the photon energy.[6] For the I channel, we have $\bar{E}_{int}/E_{avl} = 0.52$ both at 279.71 nm and at 304.67 nm, comparable to the previous results at 248 and 304.67 nm. These mean that the energy partitioning $\bar{E}_{int}/E_{avl}$ is also insensitive to the wavelength for the I channel.

3.2. Photodissociation of i-C_3H_7I. The enlarged TOF spectra of the iodine photofragment from i-C_3H_7I at 281.73, 304.02, 279.71, and 304.67 nm are shown in Figure 5a−d, respectively. The polarization of laser for these results is also parallel to the acceleration field. The corresponding translational energy distributions of photofragments have been displayed in Figure 6a−d, respectively. At 281.73 nm only (Figures 5a and 6a), we can get some partially resolved small vibrational peaks with separation of about 352 cm^{-1}, corresponding to the vibrational frequency 364 cm^{-1} of the $HC(CH_3)_2$ out-of-plane bending of the i-C_3H_7 free radical.[31,32] The results suggest that the $HC(CH_3)_2$ out-of-plane bending mode of the fragment i-C_3H_7 could be excited more easily. The reason might be, as discussed for n-C_3H_7I, that the α-carbon experiences the strongest force and the three atoms attached to the α-carbon also experience some strong effect during the C−I bond breaking of i-C_3H_7I. We also give some quantum numbers v of the $HC(CH_3)_2$ out-of-plane bending mode to those small peaks in Figures 5a and 6a to show the extent of the internal energy excitation. Different from n-C_3H_7I, no vibrational peaks can be partially resolved for the I channel at 279.71 and 304.67 nm for i-C_3H_7I. The main reason is that the lower vibrational frequency 364 cm^{-1} of the i-C_3H_7 radical (<530 cm^{-1} of n-C_3H_7) and the higher E_{avl} for the I channel require a higher resolution of the apparatus. For 304.02 nm, the signal-to-noise ratio is much lower than those at other wavelengths. Although the spectrum is accumulated over 180 000 laser shots, the signal-to-noise ratio is still not so good.

The values of energy partitioning for the photodissociation of i-C_3H_7I, from present experiments and the literature, are

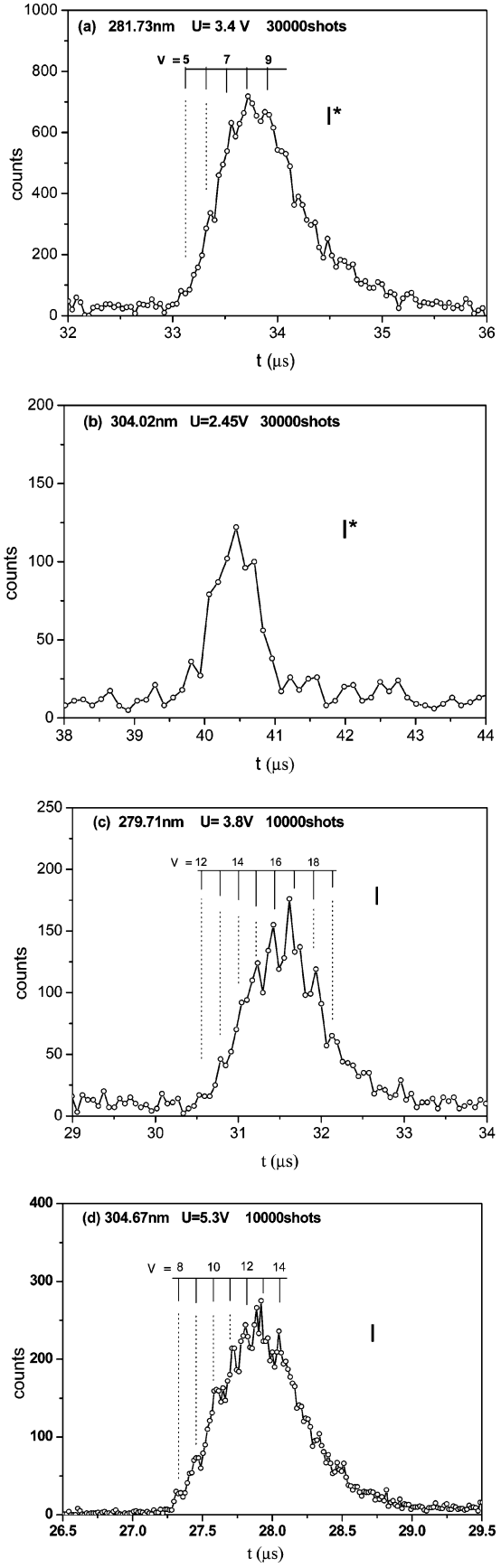

Figure 3. Enlarged TOF spectra of ionized iodine from *n*-C_3H_7I photodissociation: (a) 281.73 nm/I* (repeller $U = 3.4$ V, channel width 40 ns, 30 000 laser shots); (b) 304.02 nm/I* ($U = 2.45$ V, channel width 128 ns, 30 000 shots); (c) 279.71 nm/I ($U = 3.8$ V, channel width 64 ns, 10 000 shots); (d) 304.67 nm/I ($U = 5.3$ V, channel width 16 ns, 10 000 shots).

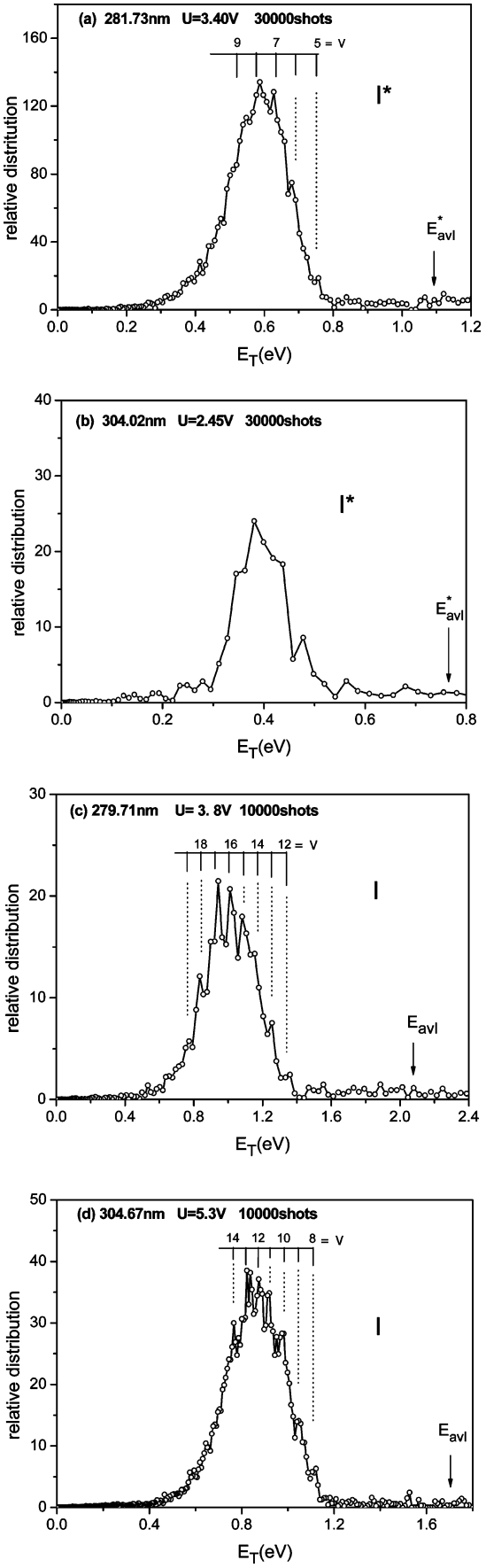

Figure 4. Translational energy distribution of the photofragments from *n*-C_3H_7I: (a) 281.73 nm/I*; (b) 304.02 nm/I*; (c) 279.71 nm/I; (d) 304.67 nm/I.

TABLE 1: Energy Partitioning in the Photodissociation of n-C_3H_7I at Various Wavelengths (D_0 = 2.363 eV[26])

wavelength (nm)	channel	E_{avl} (eV)	$\bar{E}_T$ (eV)	$\bar{E}_{int}/E_{avl}$[f]	β
248[a]	I*	1.69	0.88	0.49	(1.75)
248[b]		1.69	0.89	0.47	
266[c]		1.35	0.72	0.47	
281.73[d]		1.09	0.57	0.48	1.68
304.02[d]		0.77	0.39	0.49	~2.00
304.02[e]		0.77	0.41	0.47	
248[a]	I	2.64	1.12	0.58	(1.75)
248[b]		2.64	1.24	0.53	
279.71[d]		2.07	0.99	0.52	~2.00
304.67[d]		1.71	0.83	0.52	1.57
304.67[e]		1.71	0.80	0.53	

[a] Reference 26. [b] Reference 5. [c] Reference 2. [d] This work. [e] Reference 6. [f] The $\bar{E}_{int}/E_{avl}$ values from the literature are changed using D_0 = 2.363 eV.

shown in Table 2. At 266 nm, Riley et al.[2] gave $\bar{E}_{int}/E_{avl}$ = [0.47] for the I* channel and $\bar{E}_{int}/E_{avl}$ = [0.67] for the I channel approximately. At 248 nm, $\bar{E}_{int}/E_{avl}$ = 0.43 for the I* channel from Godwin et al.[26] is smaller than $\bar{E}_{int}/E_{avl}$ = 0.63 from Zhu et al.[5] The result of Zhu et al. might be more reliable because the two channels I* and I were resolved clearly in their TOF spectrum. From the present experiments, for the I* channel, $\bar{E}_{int}/E_{avl}$ is 0.61 at 281.73 nm and 0.65 at 304.02 nm, comparable with the result 0.63 at 248 nm from Zhu et al. For the I channel at 279.71 nm, the $\bar{E}_{int}/E_{avl}$ value is 0.62, comparable with the result at 248 nm. However, for the I channel at 304.67 nm, the $\bar{E}_{int}/E_{avl}$ value is 0.49, smaller than the results at other wavelengths. The reason of this smaller value is not clear yet.

All the experimental values $\bar{E}_{int}/E_{avl}$ = 0.47−0.65 of both propyl iodides are much larger than those $\bar{E}_{int}/E_{avl}$ = 0.11−0.18 of methyl iodide and $\bar{E}_{int}/E_{avl}$ = 0.22−0.39 of ethyl iodide. The reason is that the larger the radical size, the more the degree of freedom in vibrational modes, and the more the internal energy to be excited. This has been discussed not only with the statistical model but also with the impulsive soft model.[2]

3.3. Potential-Energy-Surface Crossing. The A band absorption of alkyl iodides involves three different transition states $^3Q_1$, $^3Q_0$, and $^1Q_1$ forming three repulsive potential-energy surfaces in the potential energy diagram. The $^3Q_0$ and $^1Q_1$ potential-energy-surfaces cross each other. The transition from the ground state X to the excited state $^3Q_0$ ($^3Q_0 \leftarrow X$) is a parallel transition; i.e., the transition dipole moment is parallel to the C−I bond. The excited state $^3Q_0$ produces adiabatically the I*($^2P_{1/2}$) state by direct dissociation and correlates nonadiabatically with the I ($^2P_{3/2}$) state by a potential-energy-surface crossing from$^3Q_0$ to $^1Q_1$. The $^3Q_1 \leftarrow X$ and $^1Q_1 \leftarrow X$ transitions are both perpendicular transitions; i.e., the transition dipole moment is perpendicular to the C−I bond and associates adiabatically with the I ($^2P_{3/2}$) state. For n-C_3H_7I and i-C_3H_7I, the A band absorption spectra of the three excited states ($^3Q_1$, $^3Q_0$, and $^1Q_1$) have not been reported separately. However, the structure of the three potential-energy surfaces would be similar for all alkyl iodides. The MCD (magnetic circular dichroism) and absorption spectra in the A band of CH_3I, C_2H_5I, and t-C_4H_9I reported by Gedanken[33] can be used for qualitative analysis of the experimental results of n-C_3H_7I and i-C_3H_7I.

For the wavelengths near 280 and 304 nm in this study, the $^1Q_1 \leftarrow X$ transition cannot be reached. In Figures 3−6, all spectra come from the initial parallel transition $^3Q_0 \leftarrow X$ because the laser light is kept polarized parallel to the acceleration field. The signals of the I* photofragment at 281.73 and 304.02 nm come from the $^3Q_0$ state adiabatically. However, the signals of the I photofragment at 279.71 and 304.67 nm come from a potential-energy-surface crossing $^3Q_0 \rightarrow {}^1Q_1$ after the initial excitation $^3Q_0 \leftarrow X$.

Near 280 nm, the signal intensity of I* at 281.73 nm is stronger than that of I at 279.71 nm, but near 304 nm, the signal intensity of I* at 304.02 nm is much weaker than that of I at 304.67 nm, for both propyl iodides. It seems that the probability of potential-energy-surface crossing near 304 nm is much larger than that near 280 nm. This can be explained by the Landau−Zener equation. As the excitation energy near 304 nm is lower than that near 280 nm, the bond dissociation velocity passing the potential-energy-surface-crossing region for 304 nm excitation is slower than that for the 280 nm excitation. Then, the time passing the potential-energy-surface-crossing region is longer and the probability of potential-energy-surface crossing is larger near 304 nm than those near 280 nm. In the consideration of ionization cross sections of I* and I, the results of the above analysis will be affected to some extent.

We have also performed the experiments with the polarization of the laser perpendicular to the acceleration field for n-C_3H_7I and i-C_3H_7I at all four wavelengths. All the TOF spectra at four wavelengths are much weaker than those of parallel polarization. These results suggest that the excitation to $^3Q_1$ state is much weaker than the excitation to $^3Q_0$ state and the lifetime of $^3Q_0$ state is much shorter than its rotational period for the mother molecule. The values of the anisotropy parameter β for both propyl iodides at four wavelengths have been calculated using eq 7 and are listed in Tables 1 and 2.

$$\beta = \frac{I_{||} - I_{\perp}}{0.5I_{||} + I_{\perp}} \tag{7}$$

β is the anisotropy parameter, $I_{||}$ is the intensity of the spectrum with the laser polarization parallel to the acceleration field, and $I_{\perp}$ is the intensity of the spectrum with the laser polarization perpendicular to the acceleration field. The β values in Tables 1 and 2 are very close to 2. This reveals that at these four laser wavelengths, the transition dipole of each propyl iodide is parallel to the C−I bond, the lifetime of the $^3Q_0$ transition state is shorter than the rotational period, and the dissociation process is direct and repulsive.

It is interesting to note that both the RCH_2 deformation mode for n-C_3H_7 and the $HC(CH_3)_2$ out-of-plane bending mode for i-C_3H_7 are the "symmetric bendings" of the three remaining bonds of the α-carbon. Just as for the "umbrella" vibrational mode for CH_3,[3,7,11,20,23] the "symmetric bendings" are usually found to be the most easily excited vibrational mode in the photodissociation of alkyl iodides in the A band. Here, a qualitative analysis on the mechanism is given in detail. During the direct photodissociation process, the propyl iodide molecule in the ground state absorbs a photon and is promoted quickly to the excited state in the A band (a couple of femtoseconds). The lifetime of the excited state is very short (about 10−20 fs), less than a vibrational period. The molecule dissociates quickly through the direct, repulsive C−I bond breaking. During the C−I bond breaking, the α-carbon experiences a strong repulsive force and moves toward the center of the three directly attached atoms. Thus it will initiate the "symmetric bending" and the "symmetric stretching" of the three remaining bonds of the α-carbon. As the "symmetric bending" frequency is generally lower than the "symmetric stretching" frequency for unhalogenated propyl radicals, the "symmetric bending" mode is excited more easily than the "symmetric stretching" mode. The time of the C−I bond breaking process (tens of femtoseconds) is much shorter than the time of the internal vibrational

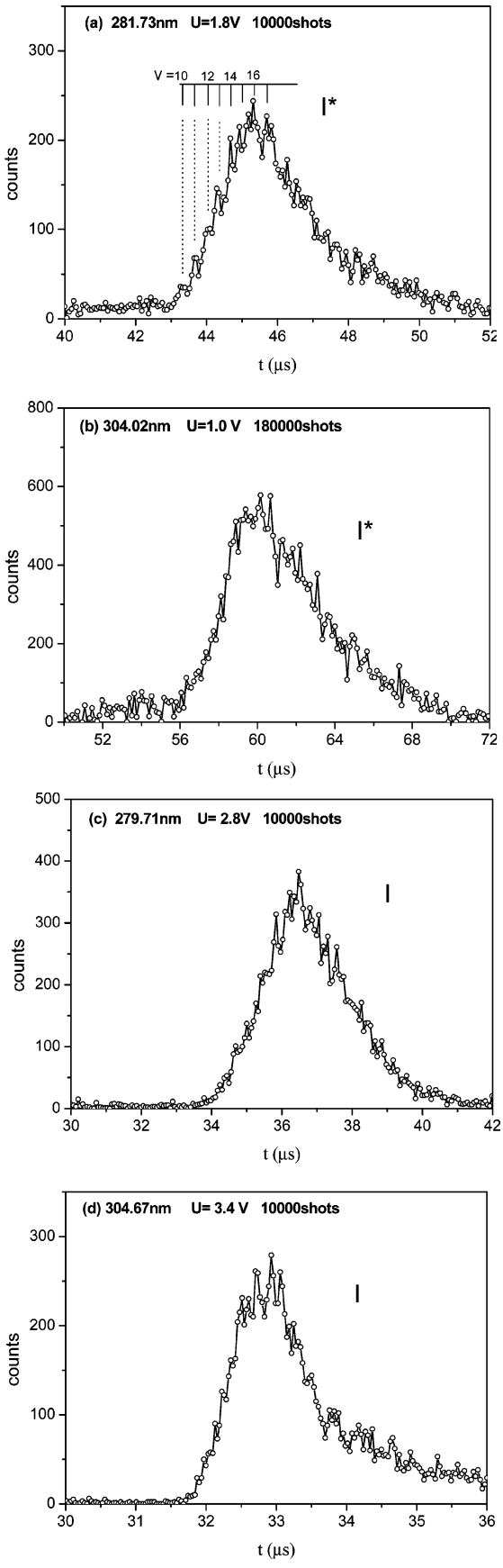

Figure 5. Enlarged TOF spectra of ionized iodine from *i*-C_3H_7I photodissociation: (a) 281.73 nm/I* (repeller $U = 1.8$ V, channel width 64 ns, 10 000 laser shots); (b) 304.02 nm/I* ($U = 1.0$ V, channel width 128 ns, 180 000 shots); (c) 279.71 nm/I ($U = 2.8$ V, channel width 64 ns, 10 000 shots); (d) 304.67 nm/I ($U = 3.4$ V, channel width 32 ns, 10 000 shots).

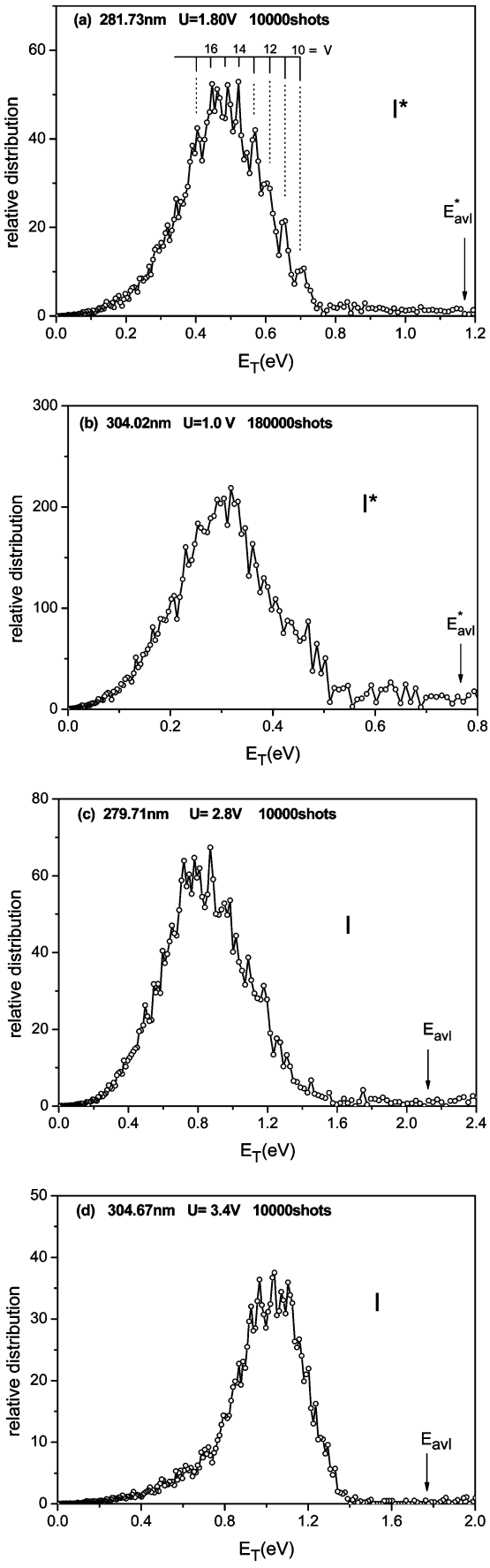

Figure 6. Translational energy distribution of the photofragments from *i*-C_3H_7I: (a) 281.73 nm/I*; (b) 304.02 nm/I*; (c) 279.71 nm/I; (d) 304.67 nm/I.

TABLE 2: Energy Partitioning in the Photodissociation of i-C_3H_7I at Various Wavelengths (D_0 = 2.296 eV[26])

wavelength (nm)	channel	E_{avl} (eV)	$\bar{E}_T$ (eV)	$\bar{E}_{int}/E_{avl}$[e]	β
248[a]	I*	1.76	1.01	0.43	(1.9)
248[b]		1.76	0.64	0.64	
266[c]		1.42	0.82	[0.42]	
281.73[c]		1.16	0.45	0.61	1.72
304.02[c]		0.84	0.29	0.65	1.75
248[a]	I	2.70	1.06	0.61	(1.9)
248[b]		2.70	0.98	0.64	
266[d]		2.36	0.82	[0.65]	
279.71[c]		2.14	0.81	0.62	1.32
304.67[c]		1.77	0.96	0.49	1.31

[a] Reference 26. [b] Reference 5. [c] This work. [d] Reference 2. [e] The $\bar{E}_{int}/E_{avl}$ values from the literature are changed using D_0 = 2.296 eV.

redistribution (~1 ps). Therefore, the "symmetric bending" mode would be the only excited vibrational mode during bond breaking and gives vibrational peaks with separation corresponding to its vibrational frequency in TOF spectra. After the bond breaking, the structure of the C_3H_7 free radical may change and the vibrational energy may be redistributed, but these will not affect the TOF spectrum of iodine and the photofragment translational spectrum.

4. Conclusion

The photodissociation of n-C_3H_7I and i-C_3H_7I has been studied at four wavelengths (281.73 and 304.02 nm for the I* channel and 279.71 and 304.67 nm for the I channel) with our mini-TOF photofragment translational spectrometer. For n-C_3H_7I, we have obtained partially resolved vibrational peaks in the TOF spectra at three wavelengths (281.73, 279.71, and 304.67 nm). These results show that the RCH_2 deformation vibration (530 cm^{-1}) of the n-C_3H_7 radical is the most easily excited vibrational mode. For i-C_3H_7I, the vibrational peaks are partially resolved only at 281.73 nm. The $\bar{E}_{int}/E_{avl}$ values for n-C_3H_7I at four wavelengths are ~0.50, comparable with the previous results. For i-C_3H_7I, the $\bar{E}_{int}/E_{avl}$ values for the I* channel at two wavelengths and for the I channel at 279.71 nm are all ~0.62, comparable with the previous results at 248 nm. However, the $\bar{E}_{int}/E_{avl}$ value for the I channel at 304.67 nm is only ~0.49. All the obtained values of β are ~2; i.e., all dissociation processes at four wavelengths originate from the $^3Q_0$ parallel transition.

Acknowledgment. This work is supported by the National Natural Science Foundation of China under Grant 20433080.

References and Notes

(1) Mulliken, R. S. *J. Chem. Phys.* **1940**, *8*, 382.
(2) Riley, S. J.; Wilson, K. R. *Faraday Discuss. Chem. Soc.* **1972**, *53*, 132.
(3) Eppink, A. T. J. B.; Parker, D. H. *J. Chem. Phys* **1998**, *109*, 4758.
(4) Hertz, R. A.; Syage, J. A. *J. Chem. Phys.* **1994**, *100*, 9265.
(5) (a) Zhu, Q. H.; Cao, J. R.; Wen, Y.; Zhang, J. M.; Zhong, X.; Huang, Y. H.; Fang, W. Q.; Wu, X. J. *Chem. Phys. Lett*, **1988**, *144*, 486. (b) Huang, Y. H.; Cao, J. R.; Wen, Y.; Zhong, X.; Zhang, J. M.; Fang, W. Q.; Wu, X. J.; Zhu, Q. H. *Acta Phys.-Chim. Sinica* **1987**, *3*, 337.
(6) Kang, W. K.; Jung, K. W.; Kim, D. C.; Jung, K. H.; Im, H. S. *Chem. Phys.* **1995**, *196*, 363.
(7) Eppink, A. T. J. B.; Parker, D. H. *J. Chem. Phys* **1999**, *110*, 832.
(8) Wu, G. R.; Jiang, B.; Ran, Q.; Zhang, J. H.; Harich, S. A.; Yang, X. M. *J. Chem. Phys.* **2004**, *120*, 2193.
(9) Aguirre, F.; Pratt, S. T. *J. Chem. Phys.* **2005**, *122*, No.234303
(10) Li, G. S.; Shin, Y. K.; Hwang, H. J. *J. Phys. Chem. A* **2005**, *109*, 9226.
(11) Felder, P. *Chem. Phys.* **1991**, *155*, 435.
(12) Person, M. D.; Kash, P. W.; Butler, L. J. *J. Chem. Phys.* **1991**, *94*, 2557.
(13) Hwang, H. J.; Elsayed, M. A. *J. Phys. Chem.* **1992**, *96*, 8728.
(14) Thoman, J. W.; Tilford, C. A.; Flesner, C. S.; Hesse, R. A. *Abstr. Pap., Am. Chem. Soc.* **1992**, *204*, 153.
(15) Taatjes, C. A.; Mastenbroek, J. W. G.; Stolte, S. *Chem. Phys. Lett.* **1993**, *216*, 100.
(16) Furlan, A.; Gejo, T.; Huber, J. R. *J. Phys. Chem.* **1996**, *100*, 7956.
(17) Kim, Y. S.; Kang, W. K.; Jung, K. H. *J. Chem. Phys.* **1996**, *105*, 551.
(18) Roeterdink, W. G.; Janssen, M. H. M. *Chem. Phys. Lett.* **2001**, *345*, 72.
(19) Aguirre, F.; Pratt, S. T. *J Chem. Phys.* **2003**, *118*, 1175.
(20) Wang, X.; Tian, Z. X.; Shi, T. J.; Shi, X. H.; Yang, D. L.; Zhu, Q. H. *Chem. Phys. Lett.* **2003**, *380*, 600.
(21) Tian, Z. X.; Bi, W. B.; Deng, H. D.; Wang, X.; Tang, Z. C.; Zhu, Q. H. *Chem. Phys. Lett.* **2004**, *400*, 15.
(22) Li, G. S.; Shin, Y. K.; Hwang, H. J. *J. Chem. Phys.* **2006**, *125*, No. 214312
(23) Lee, Y. T. Unpublished result, 1987.
(24) Li, G. S.; Hwang, H. J.; Jung, H. C. *Rev. Sci. Instrum.* **2005**, *76*, NO.023105.
(25) Bi, W. B.; Xu, X. L.; Huang, J. G.; Xiao, D. Q.; Zhu, Q. H. *Sci. China Ser. B-Chem.* **2007**, *37*, 12.
(26) Godwin, F. G.; Paterson, C.; Gorry, P. A. *Mol. Phys.* **1987**, *61*, 827.
(27) Fan, H. Y.; Pratt, S. T. *J. Chem. Phys.* **2005**, *123*, No.204301.
(28) Gedanken, A.; Robin, M. B.; Yafet, Y. *J. Chem. Phys.* **1982**, *76*, 4798.
(29) Wang, J. H.; Hsu, Y. T.; Liu, K. P. *J. Phys. Chem. A* **1997**, *101*, 6593.
(30) Pacansky, J.; Horne, D. E.; Gardini, G. P.; Bargon, J. *J. Phys. Chem.* **1977**, *81*, 2149.
(31) Pacansky, J.; Coufal, H. *J. Chem. Phys.* **1980**, *72*, 3298.
(32) Chettur, G.; Snelson, A. *J. Phys. Chem.* **1987**, *91*, 913.
(33) Gedanken, A. *Chem. Phys. Lett.* **1987**, *137*, 462.